Design and Performance Evaluation of an Actively Compliant Underwater Manipulator for Full-Ocean Depth

Dana R. Yoerger, Hagen Schempf, and David M. DiPietro
Deep Submergence Laboratory
Department of Applied Ocean Physics and Engineering
Woods Hole Oceanographic Institution
Woods Hole, MA 02543
Received December 13, 1990; accepted January 22, 1991

An underwater manipulator is described that can exhibit a wide range of compliance through a combination of mechanical design and software control and its performance characterized. The manipulator has been used in conjunction with the JASON Remotely Operated Vehicle at full-ocean depth. The major goal of the design was to produce a manipulator that can actively control the interaction forces with the work task in the hostile deep-ocean environment. The manipulator's performance has been characterized in the lab and its overall operational utility has been confirmed during tests to depths of approximately 4000 meters, including an archaeological excavation at 700 meters depth in the Mediterranean. The manipulator uses high performance brushless DC servomotors driving the joints though low-friction, zero-backlash reductions of moderate ratio consisting of cables and pulleys. Each joint is highly backdriveable and has a large range of rotation. This approach permits a variety of force control schemes such as impedance control to be implemented with no sensors other than the displacement sensors integrated with the brushless motor. It also permits high-quality torque servomechanisms to be directly implemented. This article outlines the design and illustrates the performance of a single joint in terms of friction, stiffness, and in implementing variable compliance and as a closed-loop torque servo.

海中マニピュレータは、機械設計とソフトウェア制御の組み合せとその性能を特徴付けることにより幅広い応用性を示すものと、説明できる。 マニピュレータは、深海中のJANSON Remotely Operated Vehicleに接続されて使われてきた。

この設計の主たる目的は、対向する深海環境において作業による相互作用力を動的に制御出来るマニピュレータを作ることである。 このマニピュレータの性能は、研究室レベルで明らかにされており、その全般的な運用上の効用は、地中海の深度７００メートルにおける考古学の発掘調査を含む３０００メートルを超える深度までのテストで確認されている。

マニピュレータは、ジョイント駆動に高性能のブラッシレスＤＣサーボモーターを使用し、さらにケーブルとプーリーで構成された普通の伝達装置に低摩擦、

Journal of Robotic Systems 8(3), 371–392 (1991).
 CCC 0741-2223/91/030371-22$04.00

ゼロ・バックラッシュのものを用いている。 各ジョイントは、後方での操作性もよく、また広い回転角を持っている。 この試みは、ブラッシレス・モーター周辺のセンサーの取外しのようなセンサーの装着無しでのインピーダンス制御など様々な力の制御法を可能にする。 これはまた、高性能トルク・サーボモーターの直接装着を可能にしている。

この論文では、設計の概要を表し、ジョイント単体の性能を摩擦、剛さ、可変コンプライアンスの方面及び閉ループ・トルク・サーボとして解説している。

INTRODUCTION

Most underwater manipulators have been designed for high strength and are controlled in either position or velocity. Generally, the manipulators are not backdriveable and have been specifically designed to be unresponsive to loads imposed by the task.

This basic approach is appropriate for many applications of underwater manipulators, primarily in the offshore oil and gas industry. Operators have understandably placed a high priority on making the subsea work environment (such as a wellhead or subsea completion) as "friendly" to the remotely operated vehicle (ROV) and manipulators as possible. Features such as fixtures that permit the vehicle to dock rigidly to the environment and special purpose tools permit many tasks to be completed successfully without sophisticated manipulator control. Typical tasks include turning valves, cleaning, nondestructive testing, and attaching guide wires. Most of these tasks require very large forces and moments.

The application of remotely operated or autonomous vehicles to unstructured tasks such as those encountered in scientific operations presents different manipulation requirements. An example is the JASON ROV that has been developed at the Woods Hole Oceanographic Institution (Fig. 1). The primary manipulation tasks for JASON include sampling of rocks, sediments, benthic animals, and archaeological artifacts. These tasks typically require much less strength than typical commercial offshore tasks, but they require that interaction forces be finely controlled.

Systems like JASON must typically operate in unprepared environments. In the deep ocean there are no structures with which to dock, and landing on the bottom often obscures the operators view by kicking up clouds of sediment. The preferred method of manipulation is to hover with the vehicle and operate the manipulator in a coordinated fashion. As the hover control of the vehicle will never be perfect, automatic regulation of contact forces and torques is essential.

This scenario shares many attributes with a manipulation task for an autonomous underwater vehicle. The ability to regulate contact forces and torques is especially important when a skilled operator cannot apply his or her superior visual skills and detailed understanding of manipulation processes to allow sophisticated tasks to be accomplished with a relatively simple device.

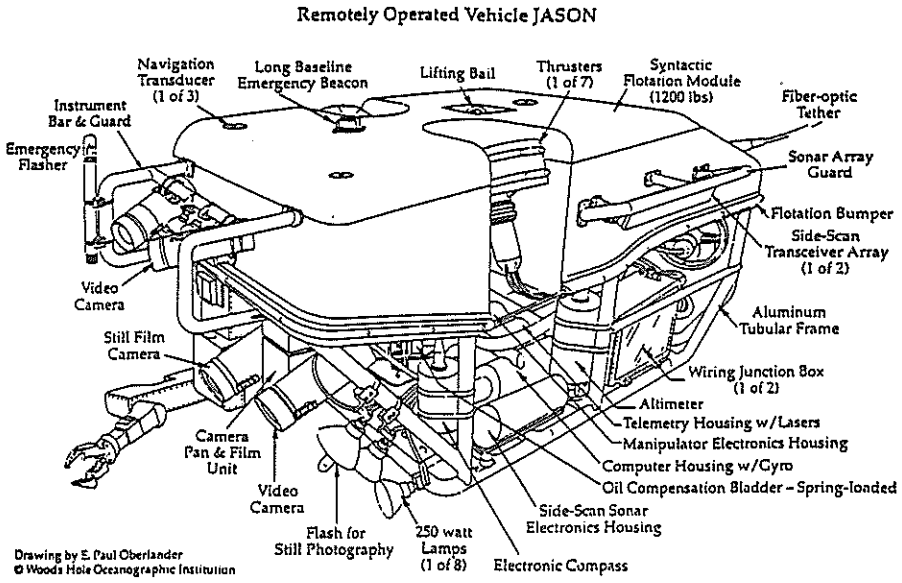

Figure 1. The remotely operated vehicle JASON is designed for scientific research of the seafloor to depths of 6000 meters. Sophisticated manipulation capability is required for sampling and the operation and recovery of instruments.

These considerations and the capabilities of JASON led to the specification of JASON's manipulator. The technical design criteria were to maximize the ability to control low forces and torques, to match JASON's lift capability, and to provide a manipulator workspace corresponding to JASON's field of view. Practical requirements included the ability to function at full-ocean depth (6000 meters), reliability, serviceability, and support electronics that could fit in 15-cm. (6-inch) diameter cylindrical pressure housings. JASON's modest power supply precluded traditional hydraulics and indicated the use of electric actuators.

Figures 2 and 3 show the manipulator and its workspace relative to JASON. Further detailed descriptions of the arm are given by DiPietro.[1]

The final device has performed well in laboratory tests, where its ability to implement desired levels of compliance and to perform as a closed-loop servo were carefully measured. Additionally, JASON and the manipulator were run at a depth of 700 meters on a daily basis for three weeks. The controllable compliance was the key to the successful recovery of over 40 artifacts from a shipwreck believed to date from the late fourth century with virtually no damage. Operationally, there were no failures in the reducers, which was the most speculative part of the design. In another test at 3000 meters depth, the manipulator joints functioned normally.

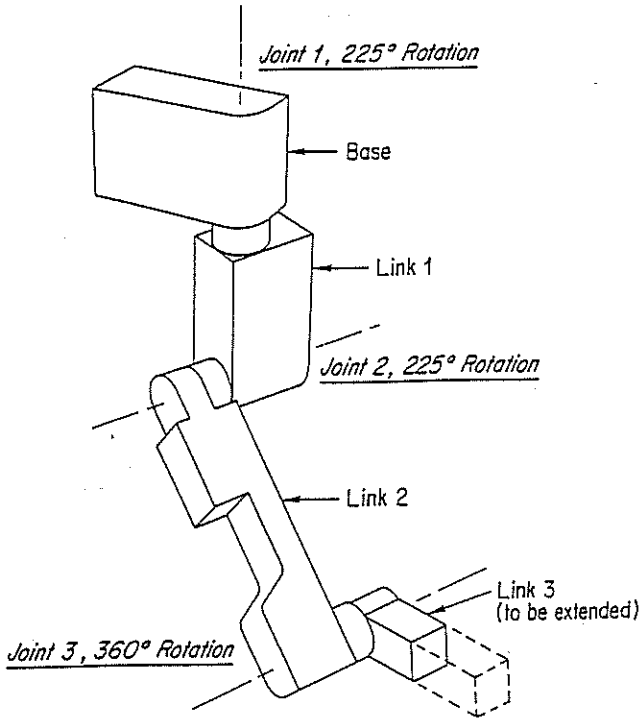

Figure 2. The original design included three rotational joints with a wide range of motion. A single-axis wrist and end-effector have been added.

DESIGN OVERVIEW

It is well established that the mechanical impedance of the endpoint of a manipulator can be controlled given ideal torque control of the joints and adequate feedback.[2,3] Given joint position and velocity feedback, the local Cartesian stiffness and damping of the end effector can be established as follows

$$\tau = \mathbf{J}^T[\mathbf{K}(\mathbf{x}_d - \mathbf{L}(\theta)) + \mathbf{B}(\dot{\mathbf{x}}_d - \mathbf{J}\dot{\theta})]$$

where the notation is as follows

τ = joint torques
θ = joint displacement vector
$\mathbf{x}$ = end effector displacement
$\mathbf{x}_d$ = desired endpoint displacement
$\mathbf{J}$ = Jacobian ($\dot{\mathbf{x}} = \mathbf{J}\dot{\theta}$)
$\mathbf{L}(\theta)$ = forward kinematics ($\mathbf{x} = \mathbf{L}(\theta)$)

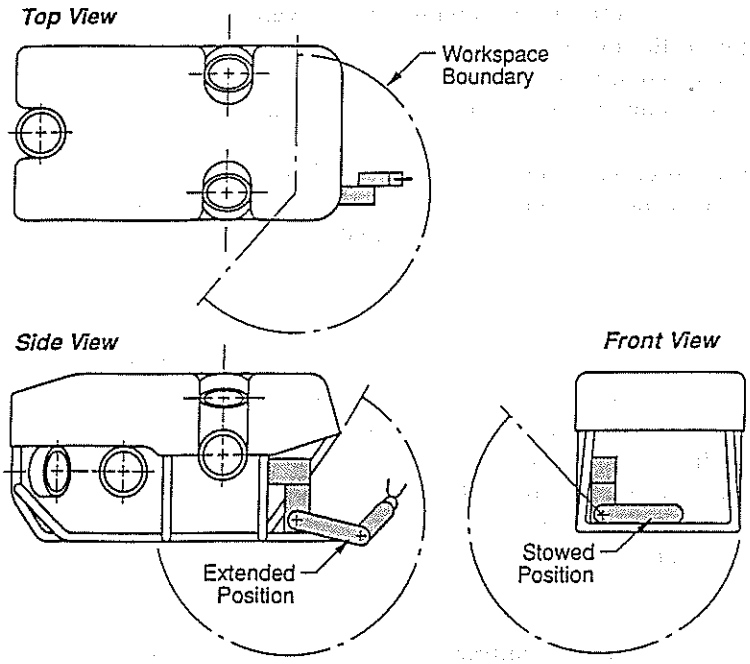

Figure 3. The workspace of the manipulator complements JASON. The end-effector can reach a large area in front of JASON, and the wide range of joint rotation also allows the manipulator to be safely stored inside JASON.

$\mathbf{K}$ = desired endpoint Cartesian stiffness
$\mathbf{B}$ = desired endpoint Cartesian damping

This simple relationship shows that a wide range of interactive behavior can be implemented given torque control of the manipulator joints and joint position and velocity feedback. Additionally, the Cartesian inertia can be set generally if the manipulator inertia matrix is known and contact forces and torques are measured.

Of these requirements, torque control of the joints is by far the most difficult to obtain. Three main approaches to this problem have been considered:

(1) Direct-drive motors
(2) Joint torque servos
(3) High dynamic range torque motors with low-friction, zero-backlash reducers.

The first choice, direct-drive motors, was eliminated in this application for several reasons. First, their large ripple torque characteristics make feedforward torque control difficult without elaborate compensation schemes. Sec-

ond, the drive electronics for commercially available units were unsuitable for packaging in the limited space available in JASON's pressure housings. The high current required to produce a given joint torque was also a problem for a vehicle with limited power, and the large size and weight of such motors was also unattractive.

The second choice, joint torque servos, is feasible and has some attractive qualities. Closing a torque loop around the entire joint (motor and reducer) could conceivably allow the use of a high reduction drive that does not have ideal characteristics such as a harmonic drive or spur gears. Use of a high reduction could permit a very compact joint assembly to be designed.

Joint torque servos using impure reductions have two major weaknesses. Regardless of the quality of the actuator and sensor, high performance torque control can be difficult to achieve because of nonlinearities in the reducer such as backlash, friction, and nonlinear compliance. Recent results[4] confirm that typical reducers place fundamental limitations on joint torque servo performance. Second, the compliant behavior of the arm would be totally dependent on the joint torque feedback. Complete reliance on a full-ocean depth torque sensor was deemed very undesirable.

The third approach, high performance motors mated to clean reducers, was chosen. Given good open-loop torque control of the motor and a reasonably pure reducer, generalized stiffness and damping can be implemented using only position and velocity feedback from the motor. Controlled, compliant behavior can be achieved without sensing at the manipulator end-effector, which is a great advantage in a hostile environment. Low reducer friction results in a drive mechanism that is backdriveable, that is the joint will move freely when external torques are applied. Backdriveability provides the manipulator with built-in protection against overloads during the inevitable collisions between the vehicle and the environment. Recent results[4] show that proper attention to reducer design also provides large benefits if closed-loop torque servos are employed.

The major problem with this approach concerns the design of the reducer. In eliminating backlash and reducing friction, the reducer could easily become large, heavy, unreliable, or overly compliant.

Recent results show that problems associated with high performance reducers can be solved through careful design.[1,5] As implemented for the JASON manipulator, the final device has no backlash, low friction, and is sufficiently stiff that the reducers internal dynamics do not significantly reduce the overall manipulator bandwidth. As noted earlier, the reducers were found to be reliable in the recent operational tests.

UNDERWATER DESIGN CONSIDERATIONS

Design of underwater manipulators is dominated by two major factors: the corrosive and electrically conductive properties of seawater and the extremely high ambient pressure (600 kg/cm^2 or 9000 psi at JASON's design depth of 6000 meters).

In this design, all motors, sensors, and reducer elements run in oil-filled volumes that are pressurized slightly above ambient. The slight overpressure allows the seals to set properly and results in oil loss rather than seawater intrusion should a leak occur. An added benefit of an oil-filled designed is built-in lubrication of the reduction mechanism and cooling of the motors.

The pressure compensating system is completely passive. As shown in Figure 4, a spring-loaded bellows is used to provide a reservoir of oil at the desired overpressure relative to the surrounding ambient seawater environment. This technique is similar to the systems on deep-diving submersibles such as ALVIN, which is also operated by the Woods Hole Oceanographic Institution.

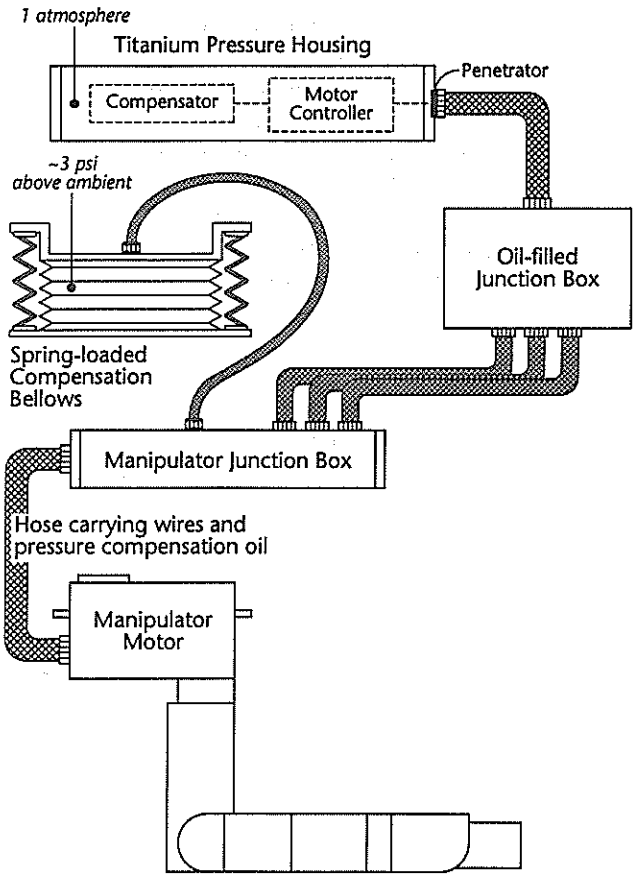

Figure 4. The manipulator is fully pressure compensated. The motors, sensors, and reducers run in an oil-filled volume slightly above ambient pressure (600 atm. or 9000 psi at 6000 meters). The oil overpressure is maintained by a spring-loaded bellows, and mineral oil was chosen as the compensating fluid. In addition to the pressure compensation, the oil also provides cooling to the motor and lubrication to the reducer and bearings.

The volume of the reservoir is large enough to accommodate compression of the oil or minor leakage.

Food-grade mineral oil was chosen for the compensating fluid for the manipulator and other major electrical systems on JASON. Mineral oil has good electrical insulating properties, has a moderate viscosity, and these properties do not change significantly with pressure. Another benefit is that mineral oil is transparent, which allows visual monitoring of the reduction mechanism during testing. Finally, the food-grade rating ensures that people working on the manipulator are not exposed to any chemical hazard.

Operation at near-ambient pressure provides several large advantages. First, the housings for the manipulator motors do not need to cope with the full ocean pressure and are thus much lighter. Second, only a low-pressure seal is required on the shaft that transmits the mechanical power from the oil-filled volume to the outside. A shaft seal capable of withstanding full-ocean pressure would have prohibitively high friction.

Before electrically commutated or "brushless" motors, pressure compensated motor operation was complicated. Arcing was exaggerated by brush "hydroplaning" and the high ambient pressure. Arcing typically would lead to oil contamination through the production of conductive particulate breakdown products, which would in turn increase arcing until the motor would fail. Some investigators have also reported production of gaseous by-products at pressure that remain in solution with the compensating fluid until pressure decreases (on return to the surface) when the gas would come out of solution, giving the motor "the bends."

Pressure-compensated motor operation has been made fairly straightforward by the advent of electronically commutated motors. Careful attention to electronic component selection and elimination of any voids in the motor windings is usually sufficient to permit successful operation. Rotor position feedback, required both to commutate the motor and for servo control, is a problem in the pressurized, oil-filled environment. Optical encoders have been used in one experimental underwater manipulator,[6] and both Hall-effect and resolvers have been used with success in underwater thruster motors. The solution chosen in this case was to use a position encoder resembling a brushless resolver that was tightly integrated with the motor, a so-called Sensorimotor.[7] These motors have operated successfully to depths of over 5000 meters with no motor failures or evidence of fluid contamination.

Proper selection of materials was required to deal with the corrosive effects of seawater. The cast portions of the links were made of A356 aluminum, an alloy with good corrosion properties. Most exposed parts that were not cast were made of 6061-T6 aluminum, which has modest strength but good corrosion resistance. One type of component, the torque tubes, requires high strength and contacts seawater at one end. These components were made of 7075-T6 aluminum, which has high strength but poor corrosion resistance. The 7075 elements were anodized. Parts internal to the reducers that do not normally contact seawater such as bearings, shafts, cables, and terminations were made of stainless steel. If the reducer should accidentally flood, the stainless

steel will be protected to some extent by being in contact with large areas of aluminum. The entire manipulator was also protected with zinc sacrificial anodes. After the three-week operational test, no significant corrosion effects were found.

MOTOR SELECTION AND PERFORMANCE

Motor requirements for this design were stringent. Technical performance requirements included high torque-to-weight ratio, good position and velocity feedback, precise torque control down to low levels, and compatibility with pressure compensated operation. Practical requirements included the ability of the drive electronics to fit in a standard JASON pressure housing and a straightforward interface to JASON's computer system.

These requirements were best met by a type of DC brushless motor called a Sensorimotor.[7] Sensorimotors resemble standard brushless motors, but they contain additional stator windings that function like a brushless resolver. They provide high quality displacement feedback that is suitable for ambient pressure operation without an external encoder. This is particularly important for a subsea design.

The motors are designed to meet high torque-to-weight requirements and the need for precise torque control. The laminated stator has 24 poles, of which four are used for sensing. The rotor contains 18 samarium-cobalt magnets, which are skewed to reduce torque ripple. Software compensation in the controller further reduces the torque ripple at low speeds to about 1%.

A digital control board was designed with a DMA interface to JASON's Instrument Bus Computer.[8] The controller includes a trajectory generator and a PID controller. For multijoint control, the controller board can also be used as a torque controller.

REDUCER AND TRANSMISSION DESIGN

Design goals for the reducers and transmissions were as follows:

(1) Compatibility with the subsea environment, pressure tolerant and corrosion resistant.
(2) Zero backlash.
(3) Low friction.
(4) Minimum size and weight.
(5) Minimum compliance across the entire range of operating torque.
(6) High fatigue life (100,000 cycles).
(7) Ease of service and maintenance.

Reductions and transmissions utilizing cables and pulleys were chosen as an attractive way to meet these design goals. Existing commercial reducers, such as planetary gears or harmonic drives, failed to meet one or more of the above criteria.

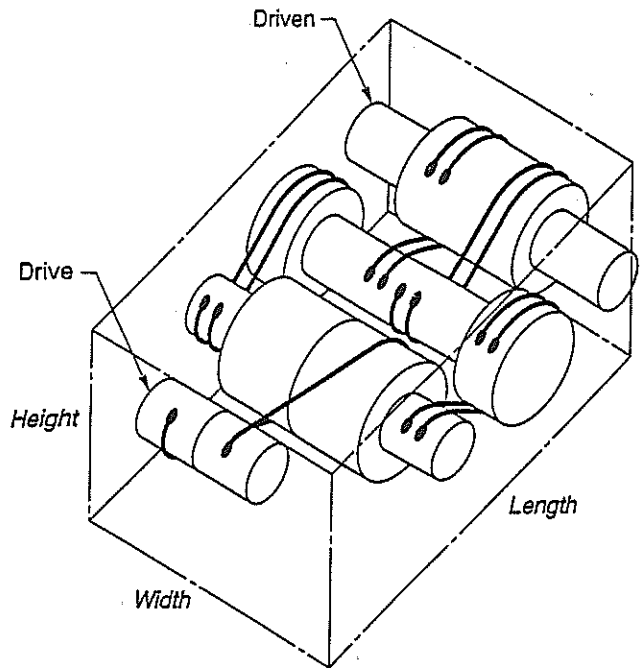

Figure 5. Schematic of the modular shoulder units. To ensure proper stiffness, four parallel cable circuits are used on the output stage, two circuits on the intermediate stage, while only one circuit is needed on the drive stage. Tensioning of all cable circuits is accomplished by a single adjustment at the drive pinion. Cable stresses are equalized through the use of looped parallel cables and split pulleys.

The design uses modular, three stage reducers for the two degrees of freedom in the shoulder, and a two stage reducer/transmission for the elbow. The use of a transmission for the elbow allows the motor and much of the first reduction stage to be located near the shoulder joint.

Figure 5 shows a schematic of the modular shoulder joints. While it was hoped to build a more integrated two-axis shoulder, compatibility with the ocean environment led to the choice of separate, modular units for each joint. Another manipulator, designed by Townsend and Salisbury[9] for in-air laboratory use, utilizes a highly integrated three-axis spherical shoulder. However, the isolation of all cables, pulleys, and bearings from seawater was considered too risky for this effort, but is a goal for future efforts.

Each modular shoulder unit includes a three-stage reduction with a ratio of 30 : 1. The ratio was chosen based on a number of factors, including the desired output torque (100 Nm), the choice of available motors, backdriveability, and

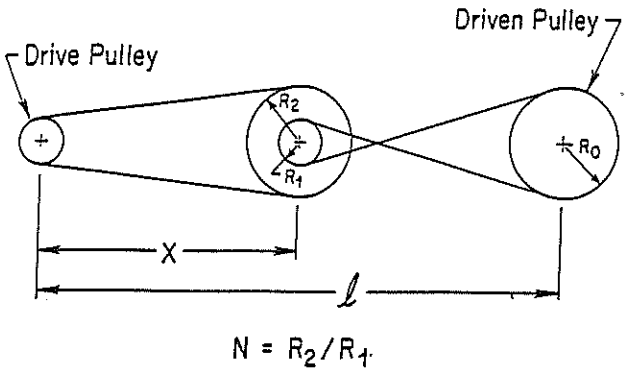

Figure 6. The elbow unit incorporates both a two-stage reducer and a transmission, which allows the motor to be positioned near the shoulder. By placing the transmission in the drive stage and putting the final reduction stage at the elbow, very little compliance is introduced by the transmission.

size. A three-stage unit was selected based on a conservative choice of minimum pulley diameter, which was driven by cable fatigue concerns.

The elbow reducer was combined with a transmission to permit the weight of the unit to be more favorably distributed back toward the shoulder (Fig. 6). As identical motors to those selected for the shoulder were used, a lower reduction of 13 : 1 was sufficient, which was implemented in two stages. The first reducer stage also serves as a transmission from the motor (located near the shoulder) down to the elbow. As the overall reducer compliance is dominated by the compliance of the last stage, the compliance of the long cables in the first stage is not significant. Details of a single reduction stage are shown in Figure 7. Below is a summary of the major design aspects.

Pretensioning

Pretensioning of the cables in the reducer stages eliminates backlash and doubles the stiffness of each stage. However, excess pretension will increase loading of the bearings and unnecessarily increase friction. In this design, pretensioning is accomplished utilizing a split pinion on the low speed end of the reducer. On each modular reducer, pretension through all stages of the reduction can be set precisely with a single adjustment using a torque wrench.

Stiffness

The stiffness of the reducers is sufficient that the first mode of each link exceeds 15 hz. As the overall reducer stiffness is dominated by the final reducer stiffness, careful design of the last stage was required. Parallel cables are used to increase stiffness without increasing cable diameter (which would reduce

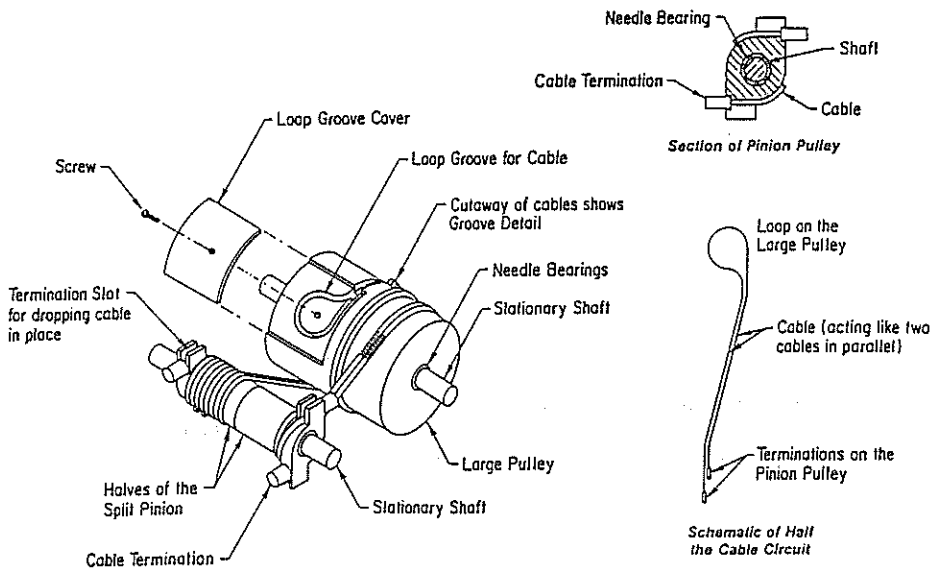

Figure 7. This illustration shows the looped parallel cable arrangement and the split drive pinion that permits the cable pretension in all circuits to be set easily and precisely.

fatigue life). The cable lengths are kept as short as possible by employing a "figure eight" cable wrap.

Friction and Stiction

A certain amount of Coulomb-type friction is unavoidable in a cable reduction.[9] The difference in tension on each side of the pulley requires that the cable slip slightly. The bearings for the pulleys will also introduce friction, so high quality roller bearings were used. Both of these factors can be minimized by carefully setting the pretension at the minimum value required to keep the cables in tension. In subsea design, the shaft seal on the reducer output shaft also introduces friction. A commercial seal with the lowest available friction (John Crane) was used.

Cable Life

Cable fatigue was a major concern in the design. Minimum pulley diameters were chosen to provide a pulley to cable diameter ratio of at least 15. The double cables were properly terminated at the small pulley, and attached to the large pulleys using a "loop groove," which was carefully designed to avoid any small diameters (Fig. 7). Adequate space on the pulleys was provided to accommodate the tendency of a cable to flatten when wrapped under tension.

SINGLE JOINT PERFORMANCE

Tests were conducted to evaluate the performance of the design in several respects. The performance of a single joint was evaluated in terms of friction and reducer compliance. The ability of the joint to act as a variable compliance element was evaluated, as was its performance in a closed-loop torque servo. All tests were conducted in air, with the joint filled with oil.

Motor Linearity

Figure 8 shows torque measured by the JR3 sensor as a function of commanded torque based on the manufacturer's published torque constant. This data shows that the motor is a good torque source with small but consistent ripple of about 1–2% of full scale. The data shows a slight directional dependence.

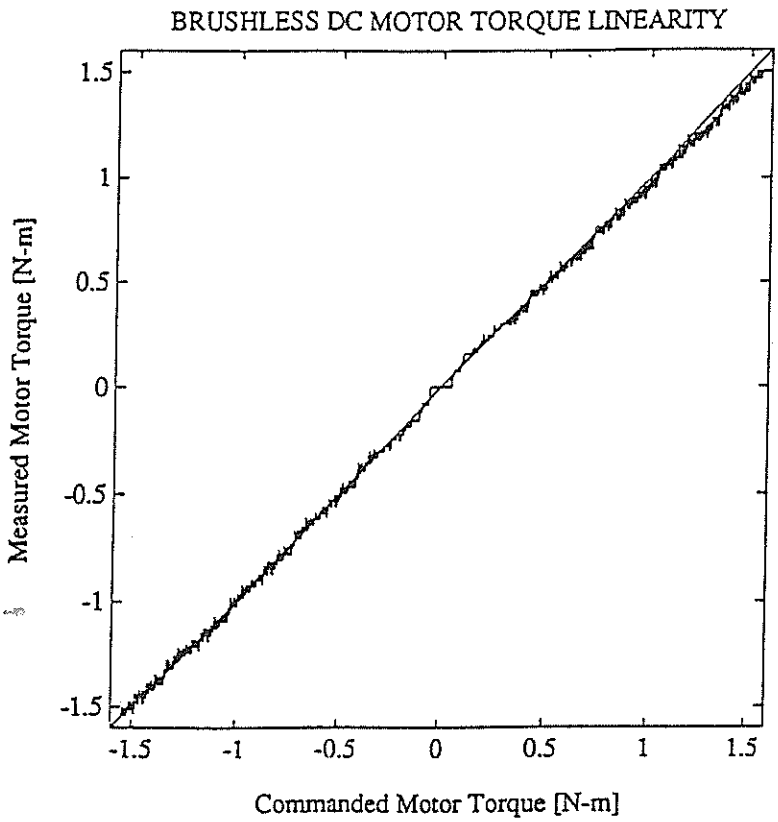

Figure 8. This plot shows motor output torque as a function of the desired torque based on the manufacturer's torque constant. Output torque was measured using a six-axis force-torque sensor.

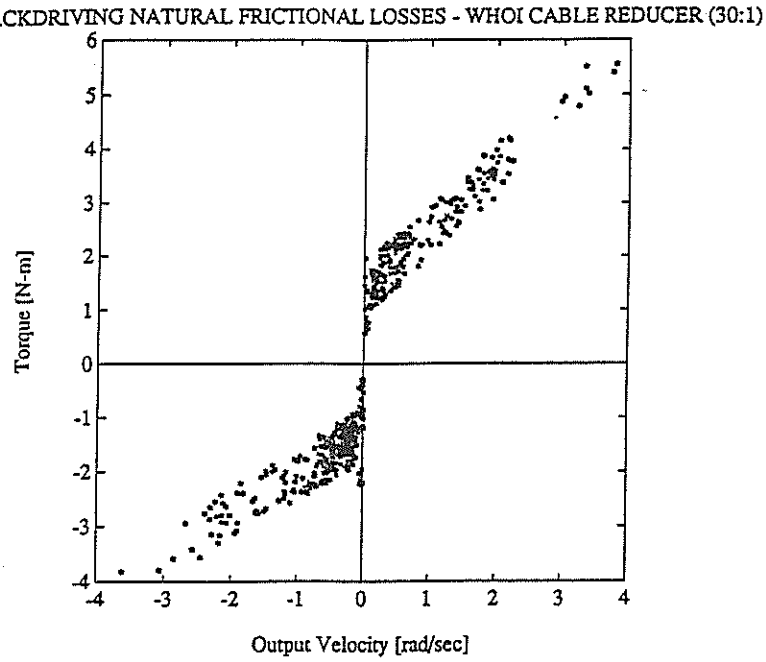

Figure 9. This plot shows the frictional losses in the reduction, as seen from the output. The output stage was driven by hand, and the velocity was inferred by a measurement at the motor, which was then transformed to units of output deflection by dividing by the reduction factor (30). The plot shows low levels of coulomb friction and stiction, and a consistent linear component. The coulomb friction level is approximately one-fourth the level reported for manipulators using harmonic drives or spur gears.

Friction

The friction present in a single shoulder joint is summarized in Figure 9. The test was run with the motor disabled and external torque applied and measured at the output with the JR3 sensor. The velocity was measured at the motor, the plotted results have been divided by the reduction ratio to correspond to velocity of the output stage. The torques were applied by hand and were slowly increased until breakaway occurred.

This test shows several important frictional characteristics of the cable reduction drive. The data was analyzed to isolate coulomb friction, linear friction, and stiction components. The linear and coulomb friction components were determined by the slope and intercept values of the best-fit line for all nonzero velocity points. The stiction value was determined as the maximum torque seen at zero velocity.

First, the pure coulomb friction component is low, approximately 1.5 Nm at the output. This compares with reported values of 8–12 Nm for a similar harmonic drive reducer[4] and approximately 8 Nm for a Puma joint utilizing spur

gears.[10] Second, the plot shows a low level of stiction, the maximum friction value before breakaway is only 1.4 times the identified coulomb friction value. The linear damping component is clearly defined, and shows slight asymmetry with respect to direction. These results show that entire joint can be backdriven with a small but consistent level of coulomb and linear friction and a low level of stiction.

Reducer Natural Stiffness

A major concern with a cable reduction is the possibility of introducing low-frequency resonant modes that can adversely effect any type of closed-loop operation. As verified by testing, careful design can result in adequate stiffness.

A test of the reducer natural stiffness was conducted by applying known torques with the motor and measuring the input deflection using the motor's built-in encoder. While stiffness could also be measured by locking the motor input and applying torque to the output, this technique was found to be more

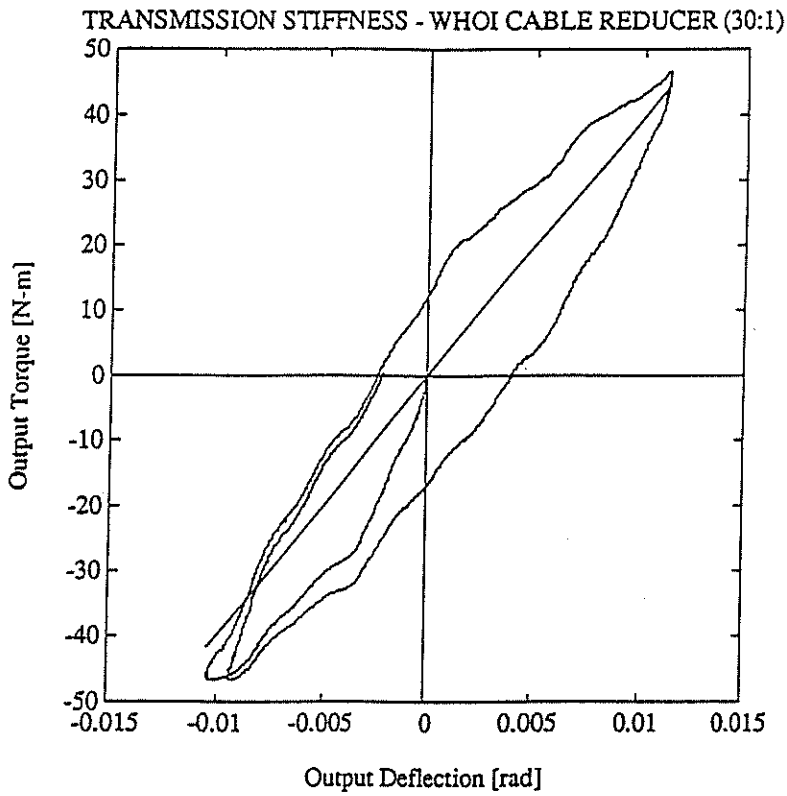

Figure 10. The stiffness of the shoulder joint is shown in this plot. The input side of the reduction was deflected by applying torque with the motor and the resulting displacement was measured using the motor position feedback.

accurate for predicting reducer-induced oscillations during closed-loop operation.[4] Figure 10 shows the motor torque plotted as a function of the input deflection for motor torques up to full scale. The plot shows that the overall stiffness is quite high with some hysteresis: the resulting resonant mode for the shoulder joint is 15 hz.

Controlling Joint Compliance without Torque Sensing

The actual implemented compliance of a single joint was measured to verify performance. The test was performed by implementing pure proportional control and slowly deflecting the joint by hand and measuring the reflected forces and moments. The JR3 force torque sensor was used to measure the moment data. The tests were conducted in air with the manipulator filled with oil. These tests reveal how the nonidealities of the motor and the reducer effect the manipulator's ability to implement various levels of compliance.

Figure 11 shows the output torque and joint output deflection for a low level of compliance, 0.21 Nm/degree, which would allow over 200 degrees of joint rotation for full motor torque. These results show that the effect of the stiction-

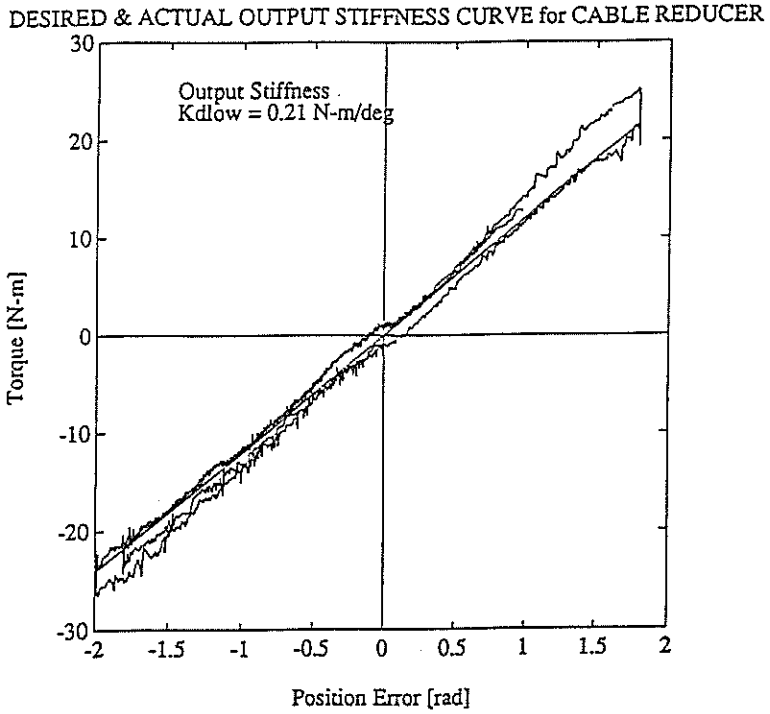

Figure 11. Output torque as function of output displacement for a low level of desired stiffness, as obtained by setting the gain of a proportional controller. The output torque was measured with the JR3 sensor, and output deflection was inferred from the motor deflection. Evidence of stiction, friction, and motor ripple can be seen.

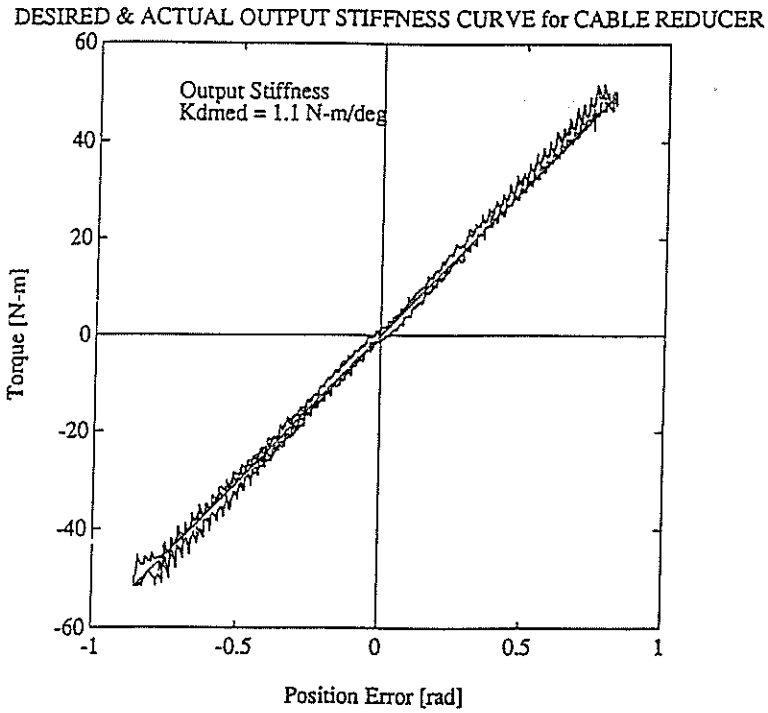

Figure 12. Output torque as function of output displacement for a medium level of desired stiffness. Compared to the previous plot, the additional loading gives rise to a displacement-dependent ripple that corresponds to complete rotations of the middle reduction stage. This implies that the ripple is caused by an eccentricity in the bearing or shaft of the middle reduction stage.

coulomb friction transition is small and that the friction band effects are repeatable in the short term. The observed ripple magnitude is small and consistent with the level observed in the motor linearity test.

Figure 12 shows the equivalent data for a higher level of stiffness, 1.1 Nm/degree, or about five times stiffer than the low compliance in the previous test. Unlike the previous test, the higher levels of torque reveal a torque ripple phenomenon that increases with loading. This torque ripple does not correspond in magnitude or spatial frequency with the motor ripple, rather its periodicity is consistent with a shaft or bearing eccentricity in the middle stage.

Figure 13 shows data from an even higher level of electronic compliance, in this case 7.5 Nm/deg or about 7 degrees output deflection for full output torque. As at the previous medium stiffness example, the nonideal behavior appears to grow at higher torque level.

Overall, these results show that the nonidealities of the joint do not prevent good implementation of various levels of compliance. The middle stage eccentricity seen in the second test illustrates the need for precision in the execution

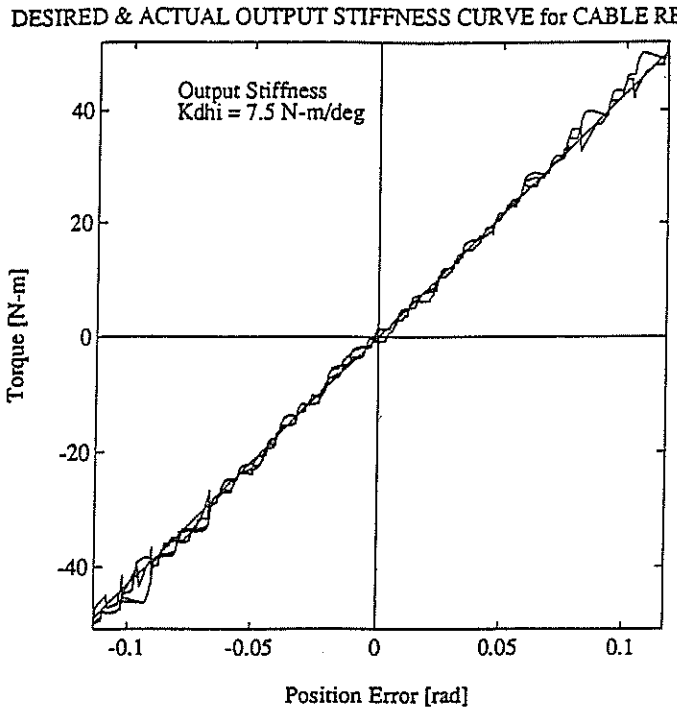

Figure 13. Output torque as function of output displacement for a high level of desired stiffness.

of these types of designs. Reducer friction, shaft seal friction, and motor ripple are evident at lower compliance levels.

Open-Loop Torque Performance

An experiment was conducted to examine the ability of a single joint to follow a small magnitude, time-varying open-loop torque command. The experiment was conducted by putting the output side of the joint in contact with the environment, then starting a torque command that consisted of a 0.5 hz sine wave 5 Nm peak-to-peak with an offset of 7.5 Nm. Given the maximum joint output of 100 Nm, the entire command occupies 5% of the entire range of torque. The command to the motor was simply the desired torque, scaled to include the static motor calibration and the reduction ratio. The JR3 sensor was used to measure the output torque, but was not used actively in the control.

Figure 14 shows the desired torque and measured output torque as functions of time. In open-loop, the dynamic torque control is not highly accurate, however the inaccuracies are fairly benign. The output trace is extremely smooth and shows no sign of stiction. The output torque shows a very slight startup transient, probably due to reducer compliance. The entire output function has

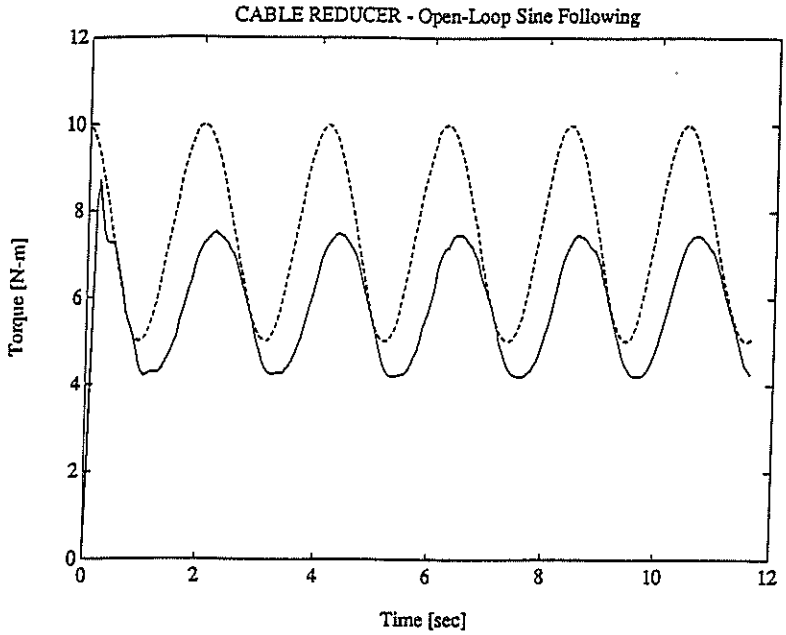

Figure 14. This plot shows open loop torque control results. The effect of reducer stiction and friction can be seen.

an offset of about 2.5 Nm, which is consistent with an estimate of the shaft seal friction loss. The output also shows a slight phase lag and magnitude reduction that can be attributed to the dynamics of the reducer.

Closed-Loop Torque Performance

While the low level of nonideal behavior of the motor and reducer permits good open loop torque control and a wide range of compliant behavior to be implemented without closing an external torque loop, the addition of an external torque measurement can allow an even higher level of performance. Figure 15 shows commanded and actual torque for a single shoulder joint utilizing a proportional-plus-integral (PI) controller. The desired torque has the same frequency, magnitude, and offset as the open-loop example. The proportional gain, K_p was chosen to yield a damping ratio of 0.7, then the integral gain K_i was selected to reduce the damping ratio of the resonant pole-pair to 0.5.

This data shows several important features of the manipulator in closed-loop torque control. First, the startup transient shows some oscillation during the commanded torque step due to compliance in the cable reduction. This transient dies out within the first second, and the system quickly acquires sinusoidal steady state. The steady response is fairly linear, but does show small oscillations caused by interaction between stiction and the integral control. The

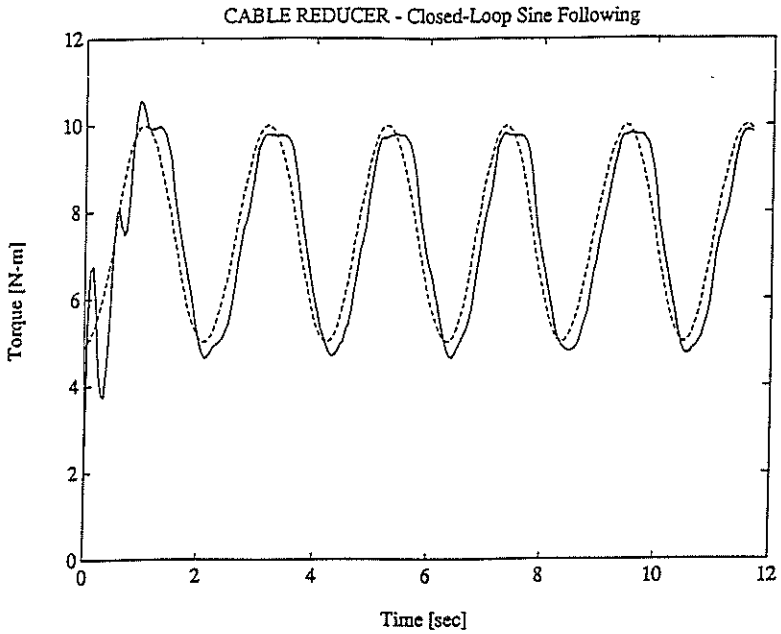

Figure 15. This plot shows closed loop torque control results. The effect of reducer stiction and friction are greatly reduced compared to the open-loop results, but some interaction between the controller's integrator and the stiction phenomenon can be seen.

level of performance is superior to equivalent examples with other reductions such as a harmonic drive or ball reducer.[4]

CONCLUSION

A manipulator has been designed and built for full-ocean depth that permits the compliance of the end effector to be controlled. The resulting device has been tested in the laboratory and its ability to actively implement a wide range of compliance has been demonstrated. At-sea tests have confirmed the operational usefulness of the controlled compliance. In three weeks of work at depths of over 700 meters, the reducers and transmissions proved reliable and stood up well to the rigors of the ocean environment. Figure 16 shows some of the objects successfully recovered from a Roman shipwreck dating from approximately 350 AD, all without damage. Another test at over 3000 meters confirmed the overall pressure tolerance of the design.

Future work with the new manipulator will move in several related directions. The manipulator control system will be integrated with the control system on the JASON vehicle to produce a unified system. Additionally, the JR3 force/torque sensor, which has already been tested to full ocean depth, will be

Figure 16. This photograph shows some of the objects from a Roman shipwreck named "ISIS" dating from the late fourth century AD that were recovered using the manipulator and the JASON vehicle. The compliant behavior of the manipulator was extremely useful in handling the objects without damage.

used in conjunction with new control algorithms to increase the range of end effector impedances that can be implemented. Also under investigation are design changes that can make these types of manipulators simpler and more compact without sacrificing performance or reliability.

Dr. J. Kenneth Salisbury originated many of the design concepts incorporated in this work and was co-advisor on Dipietro's thesis work. Dr. William Townsend, then a graduate student at MIT, also made helpful contributions to the design. Thanks to Ralph Horber at Seiberco for the motor and controller design, and Robert Ramming at JR3 for his help in the development of the full-ocean depth force-torque sensor. Chris Von Alt of WHOI provided valuable project management and advice on materials. Dr. Anna Marguerite McCann provided expertise on the archaeological excavation work. This work was sponsored by the Office of Naval Research and the Office of Naval Technology, Contracts N00014-86-C-0038, N0-00014-87-J-1111, N00014-88-K-2022. This paper is Woods Hole Oceanographic Institution Contribution number 7594.

References

1. D. M. DiPietro, "Development of an Actively Compliant Underwater Manipulator," SM Thesis, WHOI-MIT Joint Program in Oceanography and Oceanographic Engineering, December 1988.
2. J. K. Salisbury, "Active stiffness control of a manipulator in Cartesian coordinates, in *19th IEEE Conf. on Decision and Control,* Vol 1, Dec. 1980.

3. N. Hogan, "Impedance control: An approach to manipulation: Parts I, II, III.," *J. Dyn Sys, Meas, and Control*, **107,** (1985).
4. H. Schempf, "Comparative Design, Modeling, and Control Analysis of Robotic Transmission," PhD thesis, WHOI-MIT Joint Program in Oceanography and Oceanographic Engineering, August 1990.
5. W. T. Townsend and J. K. Salisbury, "The efficiency limit of belt and cable drives," *ASME J. Mechanisms, Transmissions, and Automation in Design* (1987).
6. E. Aust, E., K. H. Bohm, H. Domann, and G. F. Schultheiss, "Subsea work with robots in hyperbaric environments," in *Proc. 21st Annual Offshore Technology Conf.*, Houston, OTC 6089, May 1989.
7. W. Seitz, "A new design combining step and servo motor performances," *Electronic MOTORtechnics*, **1,** (2) (1990).
8. E. C. Mellinger, K. E. Prada, R. L. Koehler, and K. W. Doherty, "Instrument Bus: An Electronic System Architecture for Oceanographic Instrumentation," Woods Hole Oceanogr. Instit., Woods Hole, MA, Tech. Rep. WHOI-86-30, 1986.
9. J. K. Salisbury, W. Townsend, B. Eberman, and D. DiPietro, "Preliminary design of a whole-arm manipulation system (WAMS)," in *IEEE Conf on Robotics and Automation*, April, 1988.
10. B. Armstrong, "Dynamics for Robot Control: Friction Modeling and Ensuring excitation During Parameter Identification," PhD Thesis, Dept. of Electrical Engineering, Stanford Univ., 1988.